

3–4 μ m Spectroscopy of Seyfert 2 Nuclei to Quantitatively Assess the Energetic Importance of Compact Nuclear Starbursts

Masatoshi Imanishi^{1,2}

National Astronomical Observatory, Mitaka, Tokyo 181-8588, Japan

imanishi@optik.mtk.nao.ac.jp

ABSTRACT

We report on 3–4 μ m slit spectroscopy of 13 Seyfert 2 nuclei. The 3.3 μ m polycyclic aromatic hydrocarbon (PAH) emission is used to estimate the magnitudes of compact nuclear starbursts (on scales less than a few 100 pc) and to resolve the controversy over their energetic importance in Seyfert 2 nuclei. For three selected Seyfert 2 nuclei that have been well studied in the UV, the magnitudes of the compact nuclear starbursts estimated from the 3.3 μ m PAH emission (with no extinction correction) are in satisfactory quantitative agreement with those based on the UV after extinction correction. This agreement indicates that the flux attenuation of compact nuclear starburst emission due to dust extinction is insignificant at 3–4 μ m, and thus allows us to use the observed 3.3 μ m PAH luminosity to estimate the magnitudes of the compact nuclear starbursts in Seyfert 2 nuclei. Based directly on our 3–4 μ m slit spectra, the following two main conclusions are drawn: (1) except in one case, the observed nuclear 3–4 μ m emission is dominated by AGN and not by starbursts, and (2) compact nuclear starbursts are detected in 6 out of 13 Seyfert 2 nuclei, but cannot dominate the energetics of the galactic infrared dust emission in the majority of the observed Seyfert 2 galaxies. For several sources for which Infrared Space Observatory spectra taken with larger apertures and/or soft X-ray data are available, these data are combined with our 3–4 μ m slit spectra, and it is suggested that (3) extended (kpc scale) star-formation activity is energetically more important than

¹Visiting Astronomer at the Infrared Telescope Facility, which is operated by the University of Hawaii under contract from the National Aeronautics and Space Administration.

²Visiting Astronomer at the United Kingdom Infrared Telescope, which is operated by the Joint Astronomy Centre on behalf of the U.K. Particle Physics and Astronomy Research Council.

compact nuclear starbursts, and contributes significantly to the infrared luminosities of Seyfert 2 galaxies, although the AGN is still an important contributor to the luminosities, and (4) the bulk of the energetically significant extended star-formation activity is of starburst type rather than quiescent normal disk star-formation; the extended starbursts are responsible for the superwind-driven soft X-ray emission from Seyfert 2 galaxies. Finally, a correlation between the luminosities of AGNs and compact nuclear starbursts is implied; more powerful AGNs tend to be related to more powerful compact nuclear starbursts.

Subject headings: galaxies: Seyfert — galaxies: nuclei — infrared: galaxies

1. Introduction

According to the unification paradigm for Seyfert galaxies, Seyfert 1s, which show broad optical emission lines, and 2s, which do not, are intrinsically the same objects, but the nuclei of the latter class are obscured by dust along our line of sight in dusty molecular tori (Antonucci 1993). It is widely accepted that the ultimate energy source of Seyfert *nuclei* (although not of their extended host galaxies) is the release of gravitational energy caused by mass accretion onto a central supermassive blackhole (so-called AGN activity).

However, it has recently been argued that strong signatures of starbursts are detected in the nuclear UV-optical spectra of Seyfert 2 galaxies (Heckman et al. 1997; Gonzalez Delgado et al. 1998; Storchi-Bergmann et al. 2000; Gonzalez Delgado, Heckman & Leitherer 2001), and that the intrinsic extinction-corrected luminosities of compact nuclear starbursts (hereafter ‘compact’ is used to mean a size scale of less than a few 100 pc) could be comparable to the luminosities of the AGN (Gonzalez Delgado et al. 1998). In contrast, Ivanov et al. (2000) investigated the CO indices in the near-infrared *K*-band spectra of Seyfert 2 nuclei, and found no evidence for the presence of strong compact nuclear starbursts. Although these authors observed different samples of Seyfert 2 galaxies, it is nevertheless striking that they draw such contradictory conclusions on the energetic role of compact nuclear starbursts in Seyfert 2 nuclei.

According to Cid Fernandes & Terlevich (1995), compact nuclear starbursts are natural byproducts of AGNs’ dusty molecular tori. In this case, since direct UV-optical emission from the AGN is highly attenuated in Seyfert 2 nuclei, the less strongly obscured compact nuclear starburst emission will inevitably make a relatively strong contribution to the observed UV-optical fluxes in these objects. Thus, the detection of signatures of compact nuclear starbursts in the observed UV-optical spectra of Seyfert 2 nuclei (Storchi-Bergmann

et al. 2000; Gonzalez Delgado et al. 1998, 2001) would not be surprising. However, to obtain a deeper understanding of the nature of Seyfert 2 nuclei, it is certainly more important to quantify the energetic importance of compact nuclear starbursts than simply to investigate their presence. Gonzalez Delgado et al. (1998) estimated the magnitudes of compact nuclear starbursts, based on their extinction-corrected UV data, for four UV-bright Seyfert 2 galaxies, while for many other Seyfert 2 galaxies that have been studied optically, no quantitative discussions of the absolute magnitudes of compact nuclear starbursts have been made (Storchi-Bergmann et al. 2000; Gonzalez Delgado et al. 2001). Even the UV-based quantitative discussion could contain large uncertainties, because of the susceptibility of UV emission to dust extinction; the extinction correction factor for UV data may vary drastically depending on the assumed amount of dust and its spatial distribution, and has often been claimed to be quantitatively uncertain in particular applications (Baker et al. 2001). The uncertainties in the dust extinction correction are much less in the near-infrared K -band data taken by Ivanov et al. However, the spectral signatures of starbursts are weak, so that careful subtraction of old stellar and AGN emission is required to estimate the magnitudes of compact nuclear starbursts (Ivanov et al. 2000).

At 3–4 μm , we possess powerful diagnostic tools to distinguish between starburst and AGN activity, to detect weak starbursts, and to estimate the magnitudes of compact nuclear starbursts in Seyfert 2 galaxies with fewer quantitative uncertainties. As shown by Imanishi & Dudley (2000, their figure 1),

- (a) If a Seyfert 2 nucleus is powered by starbursts, strong polycyclic aromatic hydrocarbon (PAH) emission will be detected at 3.3 μm regardless of dust extinction.
- (b) If it is powered by obscured AGN activity, a carbonaceous dust absorption feature will be detected at 3.4 μm .
- (c) If it is powered by weakly obscured AGN activity, the 3–4 μm spectrum will be nearly featureless.
- (d) If it is a composite of starburst and AGN activity, the absolute luminosity and the equivalent width of the 3.3 μm PAH emission feature will be smaller than in starburst galaxies, so that these values can be used to quantitatively estimate the energetic importance of starburst activity.

Since the 3.3 μm PAH emission is intrinsically strong (Moorwood 1986; Imanishi & Dudley 2000), even the signatures of weak starbursts are detectable; even if only $\sim 10\%$ of the observed nuclear 3–4 μm flux originates in starbursts, the 3.3 μm PAH emission peak is $\sim 20\%$ higher than the continuum level, and thus is clearly recognizable in normal S/N \sim

15–20 spectra. Additionally, the effects of dust extinction are smaller at 3–4 μm than at shorter wavelengths, which makes the uncertainties in the dust extinction correction factor much smaller. This advantage is demonstrated quantitatively below. Suppose that the dust extinction in starbursts is found to be $A_V = 2\text{--}4$ mag, with an uncertainty of a factor of 2 in A_V . Since the dust extinction in the UV (~ 2000 Å) is $\sim 2.5 \times A_V$ (Savage & Mathis 1979), the corresponding dust extinction correction factor in the UV is 100–10000, differing by a factor of 100 depending on the adopted A_V . The difference becomes even larger if we go to shorter-wavelength parts of the UV region or if the actual dust extinction is larger. In contrast, since the dust extinction at 3–4 μm is $\sim 0.05 \times A_V$ (Rieke & Lebofsky 1985; Lutz et al. 1996), the extinction correction factor at 3–4 μm in the case of $A_V = 2\text{--}4$ mag is 1.1–1.2. Thus, the extinction correction is negligible at 3–4 μm , and the uncertainty in the correction factor is only at the 10% level. The high detectability of weak starbursts and the small uncertainties in dust extinction correction at 3–4 μm combine to make 3–4 μm observations a very powerful tool to quantitatively address the issue of the energetics of compact nuclear starbursts in Seyfert 2 nuclei.

This paper reports the results of 3–4 μm spectroscopy of Seyfert 2 nuclei and their implications for the energetics of these objects. Throughout the paper, $H_0 = 75$ km s^{-1} Mpc^{-1} , $\Omega_M = 0.3$, and $\Omega_\Lambda = 0.7$ are adopted.

2. Targets

The Seyfert 2 nuclei studied by Gonzalez Delgado et al. (1998, 2001) and Ivanov et al. (2000) are selected in order to be able to compare our diagnostic results at 3–4 μm directly with those previously obtained in the UV, optical, and K -band. Our particular interests are (1) to assess the quantitative reliability of the extinction correction factor based on the UV data (Gonzalez Delgado et al. 1998), (2) to make quantitative the optically based qualitative arguments on the magnitudes of compact nuclear starbursts (Gonzalez Delgado et al. 2001), and (3) to find weak compact nuclear starbursts whose presence may have been missed with K -band diagnostics (Ivanov et al. 2000). The observed sources and their properties are summarized in Table 1.

Due to our observing date (Table 2), the observed Seyfert 2 nuclei have right ascensions (R.A.) of between 7 and 16 hr. All eight Seyfert 2 nuclei in this R.A. range in Table 1 of Gonzalez Delgado et al. (2001) are observed. Ivanov et al. (2000) explicitly presented the strength of the corrected CO indices, after subtracting AGN emission, in their Table 5. In total, there are eight Seyfert 2 nuclei (Seyfert type 1.5–2.0) in the above R.A. range in the Table. Of these, NGC 5929 was in the sample of Gonzalez Delgado et al. (2001), leaving

seven independent Seyfert 2 nuclei. We attempted to observe all seven of these objects during our observing run, but could not observe UGC 6100. We started observations on Mrk 270 and Mrk 461, but based on the first few frames, found that these objects were too faint to obtain spectra of sufficient quality in a reasonable integration time; we therefore discontinued the observations. Thus, four out of the seven Seyfert 2 nuclei in Table 5 of Ivanov et al. were observed. Additionally, a 3–4 μm spectrum of the very bright Seyfert 2 nucleus NGC 1068 (R.A. = 2 hr), originally presented by Imanishi et al. (1997), is used because NGC 1068 is also in the list of Gonzalez Delgado et al. (2001).

In summary, 13 Seyfert 2 nuclei (12 sources with R.A. = 7–16 hr and NGC 1068) were observed. For the Seyfert 2 galaxies studied in the optical by Gonzalez Delgado et al. (2001), our selection should not be biased with respect to the presence or absence of compact nuclear starbursts. For the Seyfert 2 galaxies studied in the K -band by Ivanov et al. (2000), however, some bias might be present, since Seyfert 2 galaxies that are faint at 3–4 μm have been excluded. Nevertheless, our 3–4 μm study of these Seyfert 2 nuclei can provide useful information on the issue of the energetics of compact nuclear starbursts in Seyfert 2 nuclei.

3. Observations and Data Analysis

An observing log is tabulated in Table 2. Details of the observations of NGC 1068 were described by Imanishi et al. (1997), and are not repeated here. The NSFCAM grism mode (Shure et al. 1994) at IRTF on Mauna Kea, Hawaii, was used to obtain 3–4 μm spectra of all the Seyfert 2 galaxies except Mrk 273, Mrk 463, and NGC 1068. The HKL grism and L blocker were used with the 4 pixel wide slit ($= 1''.2$). The resulting spectral resolution was ~ 150 at 3.5 μm . Mrk 273 and Mrk 463 were observed with the CGS4 (Mountain et al. 1990) at UKIRT on Mauna Kea, Hawaii. The 40 1 mm^{-1} grating with 2 pixel wide slit ($= 1''.2$) was used. The resulting spectral resolution was ~ 750 at 3.5 μm . Sky conditions were photometric throughout the observations. Seeing sizes were 0''.6–0''.9 (full width at half maximum) for both the IRTF and UKIRT observing runs.

Spectra were obtained toward the flux peak at 3–4 μm . For sources observed with NSFCAM, the position angles of the slit were set along the north-south direction. Consequently, for Mrk 266, which has two nuclei lying on a southwest to northeast axis, only the southwest Seyfert 2 nucleus (Mrk 266SW; Mazzarella & Boroson 1993) was observed. For Mrk 273 and Mrk 463, which were observed with CGS4, the position angles were set at 35° and 90° east of north, respectively, so as to observe simultaneously emission from both the double nuclei with a separation of less than 5 arcsec (Scoville et al. 2000; Surace & Sanders 1999; Surace, Sanders, & Evans 2000). A standard telescope nodding technique with a throw of 12

arcsec was employed along the slit to subtract background emission. Since 3–4 μm emission from Seyfert 2 galaxies is usually dominated by compact nuclear emission (Alonso-Herrero et al. 1998), this throw is believed to be sufficiently large. Offset guide stars were used whenever available to achieve high telescope tracking accuracy. For Mrk 463, the 3–4 μm emission was dominated by the eastern nucleus (Mrk 463E) so that the obtained spectrum is almost equivalent to that of Mrk 463E only. For Mrk 273, the double nuclei were not clearly resolvable and so emission from both nuclei was combined to produce a single spectrum.

F- to G-type standard stars and one B-type star (Table 2) were observed with almost the same airmass as individual Seyfert 2 nuclei, to correct for the transmission of the Earth’s atmosphere. The L -band (3.5 μm) magnitudes of standard stars were estimated from their V -band (0.6 μm) magnitudes, by adopting the $V - L$ colors appropriate to the stellar types of individual standard stars (Tokunaga 2000).

Standard data analysis procedures were employed within IRAF³. First, bad pixels were replaced with the interpolated values of the surrounding pixels. Next, bias was subtracted from the obtained frames and the frames were divided by a flat image. The spectra of the targets and the standard stars were then extracted. Spectra were extracted by integrating signals over 4–10 arcsec along the slit (Table 3), depending on the spatial extent of the actual 3–4 μm signals. For NSFCAM data, wavelength calibration was performed using the wavelength-dependent transmission of the Earth’s atmosphere, while an argon lamp was used for the CGS4 data. The spectra of Seyfert 2 nuclei were divided by those of the standard stars, and multiplied by the spectra of blackbodies with temperatures corresponding to individual standard stars (Table 2). After flux calibration based on the adopted standard star fluxes, the final spectra were produced. NSFCAM data at \sim 3.35 μm for some sources are contaminated by an uncorrectable ghost image, and so these data points were removed.

4. Results

Flux-calibrated spectra are shown in Figure 1. The spectra of faint sources have been binned by a few spectral elements. The 3–4 μm spectra of NGC 1068 and Mrk 273, previously presented by Imanishi et al. (1997) and Imanishi & Dudley (2000) respectively, are shown again here.

³IRAF is distributed by the National Optical Astronomy Observatories, which are operated by the Association of Universities for Research in Astronomy, Inc. (AURA), under cooperative agreement with the National Science Foundation.

The possible energy sources for Seyfert 2 galaxies are AGN, compact (less than a few 100 pc) nuclear starbursts (Heckman 1999), and extended (kpc scale) star-formation in the host galaxies. The employed slit width of 1''.2 (except for NGC 1068) corresponds to the physical scale of 70–90 pc and 1.1 kpc for the nearest (NGC 3227 and NGC 5033; $z < 0.004$) and farthest (Mrk 34 and Mrk 463; $z = 0.051$) sources, respectively. Therefore, except in NGC 3227 and NGC 5033, the bulk of the compact (less than a few 100 pc) nuclear starburst emission is covered by our observations. Although extended (4–10 arcsec) emission along the slit direction is also included in our spectroscopy, the fraction of the extended emission inside this thin strip is negligible compared to the whole. Therefore, the emission directly investigated based on our slit spectra is that due to AGN and compact nuclear starburst activity, and the contamination of the emission from extended (kpc scale) star-formation activity is negligible. The slit widths employed for the UV, optical, and K -band observations are 1''.2–1''.7 (Ivanov et al. 2000; Gonzalez Delgado et al. 1998, 2001), so that these spectra also reflect the properties of the AGN and compact nuclear starburst emission. Thus, our 3–4 μm slit spectra can be directly compared with UV, optical, and K -band spectra to investigate the nature of AGN and compact nuclear starbursts.

The bulk of the AGN and compact nuclear starburst emission is, in principle, detectable in the slit. However, some flux from the compact emission could be lost in our slit spectra if the telescope tracking accuracy were insufficient. 3–4 μm emission from Seyfert 2 galaxies is generally dominated by compact nuclear emission (Alonso-Herrero et al. 1998). Thus, Table 3 compares our spectro-photometric magnitudes with photometry at 3–4 μm made with apertures of 3–9 arcsec in the literature, in order to estimate what fraction of compact nuclear 3–4 μm emission may have been missed. (We note, however, that time variability of the nuclear 3–4 μm emission may affect the comparison.) In Table 3, our slit spectrum gives a magnitude 1.2 mag fainter than the aperture photometry for NGC 5033. This is the closest source in our sample, so that it is quite plausible that a significant fraction of the 3–4 μm continuum emission has been missed in this object. However, since NGC 5033 is not used in the systematic discussion (§ 5), this missing flux for NGC 5033 will not have a significant effect on our main conclusions. With the exception of NGC 5033, the magnitude difference is less than 0.8 mag, or a factor of less than ~ 2 in all cases. This agreement within a factor of less than 2 implies that our slit spectroscopy detects at least half of the compact nuclear emission; given that aperture photometry may contain a contribution from extended emission, the actual slit loss for the compact nuclear emission is even smaller. Therefore, as far as the compact nuclear emission is concerned, the absolute 3.3 μm PAH emission fluxes measured with our slit spectra should be certain within a factor of less than 2.

To estimate the flux, luminosity, and rest-frame equivalent width of the 3.3 μm PAH emission, the spectral profile of type-1 sources (Tokunaga et al. 1991) is adopted as a template

of the $3.3 \mu\text{m}$ PAH emission. This profile can fit well the observed $3.3 \mu\text{m}$ PAH emission in some starbursts with spectra of high spectral resolution and high signal-to-noise ratios at $\sim 3.3 \mu\text{m}$ (e.g., NGC 253 and Arp 220 in Imanishi & Dudley 2000; Mrk 266SW in Fig.1). The rest-frame peak wavelength of the $3.3 \mu\text{m}$ PAH emission is assumed to be $3.29 \mu\text{m}$, and only the normalization is treated as a free parameter. The best linear fit for the data points which are affected by neither emission nor absorption is used as a continuum level. Several different continuum levels are adopted, and the uncertainties of the PAH fluxes (luminosities, equivalent widths) resulting from the continuum ambiguity are also taken into account, particularly for sources with small PAH equivalent widths. The estimated values are summarized in Table 4.

If dust grains in the obscuring material of Seyfert 2 nuclei are covered with an ice mantle, strong H_2O ice absorption should be detected (Spoon et al. 2000). This absorption feature has a peak wavelength of $3.08 \mu\text{m}$ and is spectrally broad, extending from 2.8 to $3.6 \mu\text{m}$ (e.g., Smith, Sellgren, & Tokunaga 1989). The estimates of the $3.3 \mu\text{m}$ PAH fluxes could be highly uncertain if the absorption is strong. However, most of our spectra cover $3.08 \mu\text{m}$ in the rest-frame, and yet no sign of strong H_2O ice absorption is found. The average spectrum of Seyfert 2 galaxies (Clavel et al. 2000) show no clear H_2O absorption feature either. Since the absorption strength is much weaker at $>3.25 \mu\text{m}$ than at $3.08 \mu\text{m}$ (Smith et al. 1989), possible presence of currently undetectable, weak H_2O absorption in Seyfert 2 nuclei is unlikely to affect the estimates of the $3.3 \mu\text{m}$ PAH emission significantly.

5. Discussion

5.1. What Powers the Observed Compact Nuclear $3\text{--}4 \mu\text{m}$ Emission?

The fraction of the observed nuclear $3\text{--}4 \mu\text{m}$ fluxes in our slit spectra that originates in starbursts can be estimated from the rest-frame equivalent widths of the $3.3 \mu\text{m}$ PAH emission feature ($\text{EW}_{3.3\text{PAH}}$). The $\text{EW}_{3.3\text{PAH}}$ value decreases as the AGN contribution increases (§ 1). The equivalent widths for starburst-dominated galaxies are $\sim 120 \text{ nm}$ (Moorwood 1986; Imanishi & Dudley 2000). In Table 4, only Mrk 266SW shows an $\text{EW}_{3.3\text{PAH}}$ value similar to those of starburst galaxies; we can conclude from this that only the observed nuclear $3\text{--}4 \mu\text{m}$ flux of Mrk 266SW is dominated by starbursts. Mrk 78, Mrk 273, Mrk 477, NGC 3227, and NGC 5135 all show detectable, moderately strong $3.3 \mu\text{m}$ PAH emission features, but their $\text{EW}_{3.3\text{PAH}}$ values are a factor 3–9 smaller than those of starburst galaxies. For these five sources, starbursts contribute some fraction, but less than half, of the observed nuclear $3\text{--}4 \mu\text{m}$ fluxes, and the bulk of the observed $3\text{--}4 \mu\text{m}$ fluxes originate in AGN activity. For the remaining seven Seyfert 2 nuclei (IC 3639, Mrk 34, Mrk 463, Mrk 686, NGC 1068, NGC

5033, and NGC 5929), the $\text{EW}_{3.3\text{PAH}}$ is more than a factor of 7 smaller than that expected for starburst-dominated galaxies, indicating that the predominant fraction (larger than 80%) of their 3–4 μm emission comes from AGN activity. *Our first conclusion is that, except in the case of Mrk 266SW, the observed compact nuclear 3–4 μm emission is dominated by the AGN and not by starbursts.*

This result has implications for infrared studies of AGNs. *L*- (3.5 μm) and *M*-band (4.8 μm) emission from AGNs is usually dominated by compact emission, and photometric data at these bands are used to discuss dust obscuration toward AGNs, on the assumption that this compact emission comes predominantly from the AGN and not from compact nuclear starbursts (Simpson 1998; Imanishi 2001). Our results provide supporting evidence for this assumption.

5.2. The 3.4 μm Dust Absorption Feature

The 3.4 μm carbonaceous dust absorption feature is detected in Mrk 463 and NGC 1068. The observed 3.4 μm absorption optical depths are $\tau_{3.4}(\text{observed}) = 0.042 \pm 0.005$ and 0.12 ± 0.01 for Mrk 463 and NGC 1068, respectively. In AGNs, the 3–4 μm continuum emission is dominated by dust in thermal equilibrium with a temperature of 800–1000K, close to the dust sublimation temperature, located at the innermost part of the dusty torus (Simpson 1998; Alonso-Herrero et al. 1998). The dust extinction toward the 3–4 μm continuum emitting region is thus almost the same as that toward the AGN itself. Assuming a Galactic dust model ($\tau_{3.4}/A_V = 0.004\text{--}0.007$; Pendleton et al. 1994), the dust extinction toward the AGNs is estimated to be 6–11 and 17–30 mag for Mrk 463 and NGC 1068, respectively. Mrk 463 shows a broad emission component in its near-infrared hydrogen recombination lines (Goodrich, Veilleux, & Hill 1994; Veilleux, Goodrich, & Hill 1997) so that dust obscuration toward the AGN has been suggested to be relatively modest in this object. Our result is consistent with this suggestion.

For the remaining 11 Seyfert 2 nuclei, no detectable 3.4 μm absorption feature is found. The 3.4 μm absorption feature may be suppressed if the bulk of the dust grains in the obscuring material is covered with an ice mantle (Mennella et al. 2001). However, no strong 3.08 μm ice absorption feature is found in their 3–4 μm spectra. The dust absorption feature is smeared out if less obscured starburst emission contributes significantly to the observed nuclear 3–4 μm flux (Imanishi 2000). The six sources with detectable PAH emission (Mrk 78, Mrk 266SW, Mrk 273, Mrk 477, NGC 3227, and NGC 5135) could be this case.

For the five PAH-undetected Seyfert 2 nuclei (IC 3639, Mrk 34, Mrk 686, NGC 5033,

and NGC 5929), the 3.4 μm absorption feature could remain undetectable if dust obscuration toward these AGNs is weak (§ 1). The R-value, defined as

$$R \equiv \log \frac{\nu_{3.5\mu\text{m}} F(\nu_{3.5\mu\text{m}})}{\nu_{25\mu\text{m}} F(\nu_{25\mu\text{m}})} \quad (1)$$

is a good measure for dust extinction toward AGNs (Murayama, Mouri, & Taniguchi 2000). It becomes smaller with higher dust extinction toward AGNs, and the boundary value between Seyfert 1 and 2 nuclei is estimated to be $R = -0.6$ (Murayama et al. 2000). Based on the 3.5 μm (Table 3) and *IRAS* 25 μm (Table 1) fluxes, the R-values for IC 3639, Mrk 34, Mrk 686, NGC 5033, and NGC 5929, are estimated to be -1.2 , -0.8 , -0.3 , -0.6 , and -1.2 , respectively. The R-values of Mrk 686 and NGC 5033 are in the range of Seyfert 1 nuclei, and thus weak dust obscuration is indicated, explaining the non-detection of the 3.4 μm absorption. However, IC 3639, Mrk 34, and NGC 5929 show small R-values. The non-detection could be caused by the effects of time variability or contamination from extended star-formation to the observed 25 μm flux taken with large apertures (Alonso-Herrero et al. 2001).

5.3. The Magnitudes of Compact Nuclear Starbursts as Estimated from the 3.3 μm PAH Emission Fluxes

The bulk of the UV-optical emission from the AGNs in Seyfert 2 galaxies and starbursts (Calzetti et al. 2000) is absorbed by dust and re-emitted as dust thermal emission in the infrared. Infrared (8–1000 μm) luminosities are thus used to estimate the magnitudes of AGN and starburst activity throughout this paper. Infrared (8–1000 μm) luminosities are obviously better for evaluating these kinds of activity than far-infrared (40–500 μm) luminosities because not all activity shows dust emission peaking in the far-infrared.

In starburst-dominated galaxies, the 3.3 μm PAH to far-infrared (40–500 μm) luminosity ratios ($L_{3.3\text{PAH}}/L_{\text{FIR}}$) are $\sim 1 \times 10^{-3}$ (Mouri et al. 1990). The 3.3 μm PAH to infrared (8–1000 μm) luminosity ratio ($L_{3.3\text{PAH}}/L_{\text{IR}}$) is tentatively assumed to be also 1×10^{-3} for the compact nuclear starbursts in Seyfert 2 nuclei. The scatter of the PAH-to-infrared luminosity ratio is likely to be a factor of 2–3 toward both higher and lower values around a typical value (Fischer 2000).

For IC 3639, Mrk 477, and NGC 5135, Gonzalez Delgado et al. (1998) explicitly estimated the extinction-corrected luminosities of compact nuclear starbursts, based on their UV data. The respective luminosities are 1.1×10^{43} , 1.4×10^{44} , and 4.2×10^{43} ergs s^{-1} . The infrared luminosities of the compact nuclear starbursts estimated from the observed

(extinction-uncorrected) $3.3\text{ }\mu\text{m}$ PAH emission, based on the assumption of $L_{3.3\text{PAH}}/L_{\text{IR}} \sim 1 \times 10^{-3}$, are $<1.2 \times 10^{43}$, 1.5×10^{44} , and 5.8×10^{43} ergs s^{-1} , respectively, for IC 3639, Mrk 477, and NGC 5135. It is noteworthy that the compact nuclear starburst luminosities estimated from UV data after extinction correction and from the $3.3\text{ }\mu\text{m}$ PAH emission with *no* extinction correction are in satisfactory agreement for all three sources. This agreement indicates that (1) discussions of the magnitudes of compact nuclear starbursts based on UV data after extinction correction are quantitatively reliable, (2) the extinction correction factor is not significant at $3\text{--}4\text{ }\mu\text{m}$, and (3) the assumption of $L_{3.3\text{PAH}}/L_{\text{IR}} \sim 1 \times 10^{-3}$ is reasonable. We have been concerned by the possibility that, if compact nuclear starbursts close to the central AGNs are directly exposed to X-ray emission from AGNs, PAH emission from the compact nuclear starbursts might be suppressed due to the destruction of PAHs (Voit 1992). However, the agreement suggests that this is not the case. If the bulk of the compact nuclear starbursts in Seyfert 2 nuclei occur at the outer reaches of the dusty tori around AGNs (Heckman et al. 1997), PAHs are shielded from the energetic radiation from the AGNs and thus are not destroyed, explaining the strong PAH emission from compact nuclear starbursts in Seyfert 2 nuclei. Based on these findings, the magnitudes of compact nuclear starbursts can be estimated from the observed $3.3\text{ }\mu\text{m}$ PAH emission luminosities with some confidence.

If compact nuclear starbursts energetically dominated the whole galactic infrared dust emission luminosities of Seyfert 2 galaxies, the observed $L_{3.3\text{PAH}}/L_{\text{IR}}$ ratios measured from our slit spectra should be similar to those of starburst galaxies ($\sim 1 \times 10^{-3}$). As shown in Table 4, however, none of the observed Seyfert 2 galaxies show such a large value of $L_{3.3\text{PAH}}/L_{\text{IR}}$. The differences are by a factor of 3 (Mrk 477) to larger than 10, and in most cases much larger than a factor of 2–3, the possible flux loss in our slit spectra and the intrinsic scatter of the $L_{3.3\text{PAH}}/L_{\text{IR}}$ ratios for starbursts. Therefore, *our second conclusion is that compact nuclear starbursts cannot be the dominant energy source of the whole galactic infrared dust emission luminosities in the majority of the observed Seyfert 2 galaxies*.

5.4. Comparison with Optical and K -band Diagnostic Results for Individual Sources

For the remaining ten Seyfert 2 galaxies other than IC 3639, Mrk 477, and NGC 5135, our quantitative estimates of the magnitudes of the compact nuclear starbursts are compared with qualitative arguments based on the optical and K -band data (Gonzalez Delgado et al. 2001; Ivanov et al. 2000).

Gonzalez Delgado et al. (2001) found signatures of compact nuclear starbursts (young stars) in the optical spectrum of Mrk 273. For Mrk 273, $3.3\text{ }\mu\text{m}$ PAH emission is detected; $\text{EW}_{3.3\text{PAH}}$ and $\text{L}_{3.3\text{PAH}}/\text{L}_{\text{IR}}$ are a factor of ~ 3 and ~ 10 smaller, respectively, than those of starburst galaxies. The $\text{L}_{3.3\text{PAH}}/\text{L}_{\text{IR}}$ ratio indicates that the compact nuclear starbursts explain $\sim 1/10$ of the total galactic infrared luminosity. Thus, compact nuclear starbursts are certainly present, supporting the optical results.

For Mrk 78 and NGC 1068, Gonzalez Delgado et al. (2001) found no signatures of compact nuclear starbursts, and detected only intermediate age stars in their optical spectra. For NGC 1068, only stringent upper limits are found for the $\text{EW}_{3.3\text{PAH}}$ and $\text{L}_{3.3\text{PAH}}/\text{L}_{\text{IR}}$, both of which are more than an order of magnitude smaller than those of starburst galaxies. For Mrk 78, however, $3.3\text{ }\mu\text{m}$ PAH emission is marginally detected.

For Mrk 463, Gonzalez Delgado et al. (2001) claimed that compact nuclear starbursts might be present, subject to further confirmation. No detectable $3.3\text{ }\mu\text{m}$ PAH emission is found. The upper limits for both $\text{EW}_{3.3\text{PAH}}$ and $\text{L}_{3.3\text{PAH}}/\text{L}_{\text{IR}}$ are more than an order of magnitude smaller than starburst galaxies. Compact nuclear starbursts in Mrk 463 are energetically insignificant, if they exist at all.

For Mrk 34, Gonzalez Delgado et al. (2001) found no signs of compact nuclear starbursts in the optical spectrum, with only old population stars being detected. No $3.3\text{ }\mu\text{m}$ PAH emission is detected either, supporting the conclusions based on the optical data.

Both Gonzalez Delgado et al. (2001) and Ivanov et al. (2000) studied NGC 5929 and found no evidence for strong compact nuclear starbursts. No clear $3.3\text{ }\mu\text{m}$ PAH emission is detected.

The remaining sources, Mrk 266SW, Mrk 686, NGC 3227, and NGC 5033, were studied only by Ivanov et al. (2000). They found that no strong compact nuclear starbursts are required in terms of the CO indices after correction for AGN emission. No $3.3\text{ }\mu\text{m}$ PAH emission is detected in Mrk 686 and NGC 5033, supporting their argument. However, in Mrk 266SW, the nuclear $3\text{--}4\text{ }\mu\text{m}$ emission must be dominated by starbursts, although these detected compact nuclear starbursts can explain only $\sim 10\%$ of the total galactic infrared luminosity. $3.3\text{ }\mu\text{m}$ PAH emission was also clearly detected in NGC 3227, and compact nuclear starbursts can explain $\sim 20\%$ of the whole galactic infrared luminosity. In Mrk 266SW and NGC 3227, compact nuclear starbursts are certainly present, and they explain a non-negligible fraction of the total galactic infrared luminosities. The signatures of compact nuclear starbursts may have been missed during the complicated procedures required to find their weak signatures in the K -band (Ivanov et al. 2000).

5.5. The Energetic Importance of AGN and Extended Star-Formation Activity

Since the observed nuclear 3–4 μm emission is dominated by AGN activity (§ 5.1), it would be expected that AGN activity also contributes much more than compact nuclear starbursts to the net galactic infrared (8–1000 μm) luminosities of Seyfert 2 galaxies. However, the AGN-driven infrared luminosities of these objects are difficult to estimate because they are highly dependent on the spatial distribution of dust in the dusty torus, which is poorly constrained observationally. Thus, we estimate the energetic importance of extended star-formation in the host galaxies, which is the remaining probable power source of Seyfert 2 galaxies other than compact nuclear starbursts and AGNs, by using the PAH emission. PAH emission can be produced both with starbursts and normal quiescent star-formation in a similar way (Helou et al. 2000).

To investigate the magnitude of extended (kpc scale) star-formation activity, *Infrared Space Observatory (ISO)* spectra taken with large apertures are useful. Genzel & Cesarsky (2000) summarized the *ISO* results; they found that (1) the 7.7 μm PAH to far-infrared luminosity ratios in Seyfert galaxies are similar to those of starburst galaxies, and that (2) the bulk of the PAH emission is spatially extended. Therefore, they argued that the bulk of the far-infrared emission from Seyfert galaxies originates in extended star-formation activity.

Of the 13 Seyfert 2 galaxies, Clavel et al. (2000) have presented *ISO* 2.5–11 μm spectra taken with $24 \times 24 \text{ arcsec}^2$ apertures, and quote PAH fluxes for four sources (Mrk 266, NGC 3227, NGC 5033, and NGC 5929). For these sources, the energetic importance of extended star-formation activity can be investigated by comparing the measured PAH fluxes in our slit spectra with those in the *ISO* spectra.

The effects of dust extinction are similar at 3–8 μm (Lutz et al. 1996). The 7.7 μm PAH emission is the strongest PAH emission feature. However, its flux estimates in the *ISO* spectra may be highly uncertain (Clavel et al. 2000; Laureijs et al. 2000), due to the presence of strong, spectrally broad 9.7 μm silicate dust absorption feature and insufficient wavelength coverage longward of these emission and absorption features, which make a continuum determination difficult (Dudley 1999). Quantitatively reliable flux estimates of the 3.3 μm PAH emission in the *ISO* spectra are also difficult due to the scatter in the data points at 3–4 μm (Clavel et al. 2000, their figure 8). Consequently, the 6.2 μm PAH emission, which is isolated and moderately strong, is most suitable to investigate the extended star-formation activity based on the *ISO* spectra (Fischer 2000).

The 6.2 μm PAH to infrared luminosity ratios ($L_{6.2\text{PAH}}/L_{\text{IR}}$) for starbursts are estimated to be $\sim 6 \times 10^{-3}$, with a scatter of a factor of 2–3 toward both higher and lower values (Fis-

cher 2000), where it is assumed that $L_{\text{IR}} \sim L_{\text{FIR}}$ for starbursts. The respective $L_{\text{6.2PAH}}/L_{\text{IR}}$ ratios are 4×10^{-3} , 4×10^{-3} , 3×10^{-3} , and 1×10^{-3} , for Mrk 266, NGC 3227, NGC 5033, and NGC 5929 (Clavel et al. 2000), roughly half of (Mrk 266, NGC 3227, and NGC 5033) or more than six times smaller than (NGC 5929) the typical value for systems dominated by starbursts. Since the observed $L_{\text{3.3PAH}}/L_{\text{IR}}$ ratios indicate that the compact nuclear starbursts energetically fall short of the total infrared luminosities by a factor of larger than 6 for these four sources (Table 4), it can be said that extended star-formation (but not compact nuclear starbursts) contributes significantly to the infrared luminosities of these Seyfert 2 galaxies. This statement was made by Genzel & Cesarsky (2000) for Seyfert galaxies as a whole based on the $7.7 \mu\text{m}$ PAH emission. Based on the $6.2 \mu\text{m}$ PAH emission, here, it has been confirmed that this is true also for the four individual Seyfert 2 galaxies, and probably for Seyfert 2 galaxies as a whole. The individual $L_{\text{6.2PAH}}/L_{\text{IR}}$ ratios for Mrk 266, NGC 3227, and NGC 5033 are within the scattered range of the ratios for starbursts. However, the overall trend of lower values implies that AGN activity also makes an important contribution to the infrared luminosities of Seyfert 2 galaxies.

5.6. Is Extended Star-Formation Quiescent or of Starburst Type?

While both starbursts and quiescent disk star-formation in normal galaxies can produce PAH emission (§ 5.5), strong soft X-ray emission driven by superwind is observed only if the star-formation rate per unit area exceeds a certain threshold ($10^{-1} \text{ M}_\odot \text{ yr}^{-1} \text{ kpc}^{-2}$; Heckman 2000). Starbursts surpass this threshold, while quiescent normal disk star-formation does not (Kennicutt 1998). These different characteristics can be used to understand the properties of energetically significant extended star-formation activity.

Of the 13 Seyfert 2 galaxies, Levenson, Weaver, & Heckman (2001) have estimated superwind-driven soft X-ray luminosities for eight sources (IC 3639, Mrk 78, Mrk 266, Mrk 273, Mrk 463, Mrk 477, NGC 1068, and NGC 5135), and found that, as a whole, their soft X-ray to far-infrared luminosity ratios are as high as those of starburst galaxies. Therefore, starburst activity is a significant contributor to the far-infrared emission and also to the infrared dust emission. Since compact nuclear starbursts detected in our slit spectra were found to be energetically insignificant (§ 5.3), the energetically significant starbursts must be extended. *Our third conclusion is that the bulk of the energetically significant extended (kpc scale) star-formation activity is of starburst-type and not quiescent normal disk star-formation. It is the extended (kpc scale) starbursts, rather than the compact (less than a few 100 pc) nuclear starbursts, that are responsible for the superwind-driven soft X-ray emission.* If starbursts are inevitable phenomena in Seyfert 2 galaxies, their extended starburst activity

is energetically more important than their compact nuclear starbursts. This is actually the case for the four Seyfert 2 galaxies studied in detail in the UV (Gonzalez Delgado et al. 1998) and for the famous, well-studied Seyfert 2 galaxy NGC 1068 (Le Floc'h et al. 2001).

5.7. Do More Powerful AGNs Have More Powerful Compact Nuclear Starbursts?

We test the hypothesis that more powerful AGNs might be related to more powerful compact nuclear starbursts (Gonzalez Delgado et al. 1998). Figure 2 compares the $12\ \mu\text{m}$ luminosity with the $3.3\ \mu\text{m}$ PAH emission luminosity. The total galactic $12\ \mu\text{m}$ luminosity is regarded as a measure of AGN power (Gonzalez Delgado et al. 2001). The $3.3\ \mu\text{m}$ PAH luminosities, measured with our slit spectroscopy, reflect the magnitudes of compact nuclear starbursts. The picture of Gonzalez Delgado et al. (1998) would be supported if we were to find a positive correlation between $12\ \mu\text{m}$ luminosity and $3.3\ \mu\text{m}$ PAH emission luminosity.

In Fig. 2, this trend appears to be present, although the scatter is moderately large. We apply the generalized Kendall's rank correlation statistic (Isobe, Feigelson, & Nelson 1986) to the data points in Fig. 2, and estimate the probability that a correlation is not present to be 0.11, by using the software available at the web page: <http://www.astro.psu.edu/statcodes/>. Thus, provided that the $12\ \mu\text{m}$ luminosity is a good measure of AGN power, *it is found that the luminosities of AGNs and compact nuclear starbursts in Seyfert 2 galaxies are correlated, and more powerful AGNs tend to contain more powerful compact nuclear starbursts.*

6. Summary

We performed $3\text{--}4\ \mu\text{m}$ spectroscopy of 13 Seyfert 2 nuclei that were previously studied in the UV, optical, and near-infrared K -band. Making use of the $3.3\ \mu\text{m}$ PAH emission feature detected in our slit spectra, the following results were obtained.

1. Our PAH-based, extinction-uncorrected estimates of the luminosities of compact (less than a few 100 pc) nuclear starbursts were found to agree well with those based on extinction-corrected UV data in three selected Seyfert 2 galaxies (IC 3639, Mrk 477, and NGC 5135). This agreement indicates that compact nuclear starburst emission is not significantly attenuated due to dust extinction at $3\text{--}4\ \mu\text{m}$, so that the observed $3.3\ \mu\text{m}$ PAH emission luminosity is a powerful diagnostic of the magnitudes of compact nuclear starbursts.

2. For the remaining ten Seyfert 2 galaxies, our PAH-based diagnostic results were compared with qualitative arguments based on the optical and K -band spectra. For Mrk 273, signs of compact nuclear starbursts were found, supporting the qualitative optically based argument. For Mrk 463, possible compact nuclear starbursts implied from the optical data were not confirmed at 3–4 μm . For Mrk 78 and NGC 1068, both of which show signatures of only intermediate age stars in the optical, 3.3 μm PAH emission was marginally detected in Mrk 78. Optical and/or K -band spectra show no evidence for compact nuclear starbursts in Mrk 34, Mrk 266SW, Mrk 686, NGC 3227, NGC 5033, and NGC 5929. At 3–4 μm , signatures of compact nuclear starbursts were found in Mrk 266SW and NGC 3227.
3. Quantitative estimates of the magnitudes of nuclear starbursts were made based on the observed 3.3 μm PAH emission luminosities for the 13 Seyfert 2 galaxies, and found that (1) nuclear 3–4 μm emission is dominated by AGN activity rather than by starburst activity in all Seyfert 2 galaxies but one (Mrk 266SW), and (2) compact nuclear starbursts can explain only a small fraction (<1/10–1/3) of the infrared dust emission luminosities.
4. The 3.4 μm carbonaceous dust absorption feature is detected only in the two Seyfert 2 nuclei, Mrk 463 and NGC 1068.
5. When our observations were combined with large-aperture *ISO* spectra for the four sources (Mrk 266, NGC 3227, NGC 5033, and NGC 5929), it was confirmed that extended (kpc scale) star-formation activity is energetically more important than compact nuclear starbursts, and contributes significantly to the infrared dust emission luminosities of Seyfert 2 galaxies. However, the AGNs are likely to be still important contributors to the luminosities.
6. Making use of soft X-ray data for the eight sources (IC 3639, Mrk 78, Mrk 266, Mrk 273, Mrk 463, Mrk 477, NGC 1068, and NGC 5135), it was suggested that the energetically significant extended star-formation activity is of starburst-type and not quiescent normal disk star-formation. These extended starbursts are responsible for the superwind-driven soft X-ray emission from Seyfert 2 galaxies.
7. We find evidence supporting the scenario in which more powerful AGNs are related to more powerful compact nuclear starbursts, provided that 12 μm luminosity is a good measure of AGN power.

We thank S. K. Leggett, J. Davies, T. Wold, and T. Carroll for their support during the UKIRT observing runs, and J. Rayner and B. Golisch for their support before and during

the IRTF observing run. We are grateful to Drs. K. Aoki, T. Nakajima, and Y. P. Wang for their useful comments on this manuscript, and Dr. T. T. Takeuchi for invaluable discussions about statistical tests. The anonymous referee and the scientific editor, Dr. S. Willner, gave invaluable comments, which improved this paper significantly. Spectra of Mrk 273 and Mrk 463 were obtained while MI was at the University of Hawaii. This research has made use of the NASA/IPAC Extragalactic Database (NED) which is operated by the Jet Propulsion Laboratory, California Institute of Technology, under contract with the National Aeronautics and Space Administration.

REFERENCES

Alonso-Herrero, A., Simpson, C., Ward, M. J., & Wilson, A. S. 1998, *ApJ*, 495, 196

Alonso-Herrero, A., Quillen, A. C., Simpson, C., Efstathiou, A. & Ward, M. J. 2001, *AJ*, 121, 1369

Antonucci, R. 1993, *ARA&A*, 31, 473

Baker, A. J., Lutz, D., Genzel, R., Tacconi, L. J., & Lehnert, M. D. 2001, *A&A*, 372, L37

Calzetti, D., Armus, L., Bohlin, R. C., Kinney, A. L., Koornneef, J., & Storchi-Bergmann, T. 2000, *ApJ*, 533, 682

Cid Fernandes, R. Jr., & Terlevich, R. 1995, *MNRAS*, 272, 423

Clavel, J. et al. 2000, *A&A*, 357, 839

Dudley, C. C., 1999, *MNRAS*, 307, 553

Fischer, J. 2000, in ISO Beyond the Peaks, ed. A. Salama, M. F. Kessler, K., Leech, & B. Schulz (ESA SP-456; Noordwijk: ESA), 239 (astro-ph/0009395)

Genzel, R., & Cesarsky, C. J. 2000, *ARA&A*, 38, 761

Glass, I. S., & Moorwood, A. F. M. 1985, *MNRAS*, 214, 429

Gonzalez Delgado, R. M., Heckman, T., Leitherer, C., Meurer, G., Krolik, J., Wilson, A. S., Kinney, A., & Koratkar, A. 1998, *ApJ*, 505, 174

Gonzalez Delgado, R. M., Heckman, T., & Leitherer, C. 2001, *ApJ*, 546, 845

Goodrich, R. W., Veilleux, S., & Hill, G. J. 1994, *ApJ*, 422, 521

Heckman, T. M. 1999, astro-ph/9912029

Heckman, T. M. 2000, astro-ph/0009075

Heckman, T. M., Gonzalez Delgado, R., Leitherer, C., Meurer, G. R., Krolik, J., Wilson, A. S., Koratkar, A., & Kinney, A. 1997, *ApJ*, 482, 114

Helou, G., Lu, N. Y., Werner, M. W., Malhotra, S., & Silbermann, N. 2000, *ApJ*, 532, L21

Imanishi, M. 2000, *MNRAS*, 319, 331

Imanishi, M. 2001, *AJ*, 121, 1927

Imanishi, M., & Dudley, C. C. 2000, *ApJ*, 545, 701

Imanishi, M., Terada, H., Sugiyama, K., Motohara, K., Goto, M., & Maihara, T. 1997, *PASJ*, 49, 69

Isobe, T., Feigelson, E. D., & Nelson, P. I. 1986, *ApJ*, 306, 490

Ivanov, V. D., Rieke, G. H., Groppi, C. E., Alonso-Herrero, A., Rieke, M. J., & Engelbracht, C. W. 2000, *ApJ*, 545, 190

Kennicutt, R. 1998, *ApJ*, 498, 541

Laureijs, R. J. et al. 2000, *A&A*, 359, 900

Lawrence, A., Ward, M., Elvis, M., Fabbiano, G., Willner, S. P., Carleton, N. P., & Longmore, A. 1985, *ApJ*, 291, 117

Le Floc'h, E., Mirabel, I. F., Laurent, O., Charmandaris, V., Gallais, P., Sauvage, M., Vigroux, L., & Cesarsky, C. 2001, *A&A*, 367, 487

Levenson, N. A., Weaver, K. A., & Heckman, T. M. 2001, *ApJ*, 550, 230

Lutz, D. et al. 1996, *A&A*, 315, L269

Marco, O., & Alloin, D. 2000, *A&A*, 353, 465

Mazzarella, J. M., & Boroson, T. A. 1993, *ApJS*, 85, 27

Mazzarella, J. M., Gaume, R. A., Soifer, B. T., Graham, J. R., Neugebauer, G., & Matthews, K. 1991, *AJ*, 102, 1241

Mennella, V., Munoz Caro, G. M., Ruiterkamp, R., Schutte, W. A., Greenberg, J. M., Brucato, J. R., & Colangeli, L. 2001, *A&A*, 367, 355

Moorwood, A. F. M. 1986, *A&A*, 166, 4

Mountain, C. M., Robertson, D. J., Lee, T. J., & Wade, R. 1990, *Proc. SPIE*, 1235, 25

Mouri, H., Kawara, K., Taniguchi, Y., & Nishida, M. 1990, *ApJ*, 356, L39

Murayama, T., Mouri, H., & Taniguchi, Y. 2000, *ApJ*, 528, 179

Pendleton, Y. J., Sandford, S. A., Allamandola, L. J., Tielens, A. G. G. M., & Sellgren, K. 1994, *ApJ*, 437, 683

Rieke, G. H. 1978, *ApJ*, 226, 550

Rieke, G. H., & Lebofsky, M. J. 1985, *ApJ*, 288, 618

Sanders, D. B., & Mirabel, I. F. 1996, *ARA&A*, 34, 749

Savage, B. D., & Mathis, J. S. 1979, *ARA&A*, 17, 73

Scoville, N. Z. et al. 2000, *AJ*, 119, 991

Shure, M. A., Toomey, D. W., Rayner, J. T., Onaka, P., & Denault, A. J. 1994, *Proc. SPIE*, 2198, 614

Simpson, C. 1998, *ApJ*, 509, 653

Smith, R. G., Sellgren, K., & Tokunaga, A. T. 1989, *ApJ*, 344, 413

Spoon, H. W. W., Koornneef, J., Moorwood, A. F. M., Lutz, D., & Tielens, A. G. G. M. 2000, *A&A*, 357, 898

Storchi-Bergmann, T., Raimann, D., Bica, E. L. D., & Fraquelli, H. A. 2000, *ApJ*, 544, 747

Surace, J. A., & Sanders, D. B. 1999, *ApJ*, 512, 162

Surace, J. A., Sanders, D. B., & Evans, A. S. 2000, *ApJ*, 529, 170

Tokunaga, A. T., Sellgren, K., Smith, R. G., Nagata, T., Sakata, A., & Nakada, Y. 1991, *ApJ*, 380, 452

Tokunaga, A. T. 2000, in *Allen's Astrophysical Quantities*, ed. A. N. Cox (4th ed: AIP Press: Springer), Chapter 7, p.143

Veilleux, S., Goodrich, R. W., & Hill, G. J. 1997, *ApJ*, 477, 631

Voit, G. M. 1992, *MNRAS*, 258, 841

Zhou, S., Wynn-Williams, C. G., & Sanders, D. B. 1993, *ApJ*, 409, 149

Table 1. Summary of Seyfert 2 nuclei.

Object (1)	Redshift (2)	f_{12} [Jy] (3)	f_{25} [Jy] (4)	f_{60} [Jy] (5)	f_{100} [Jy] (6)	$\log L_{\text{FIR}}$ [ergs s $^{-1}$] (7)	$\log L_{\text{IR}}$ [ergs s $^{-1}$] (8)	Remarks (9)
IC 3639	0.011	0.64	2.26	7.52	10.7	44.25	44.33	G
Mrk 34	0.051	0.07	0.46	0.81	0.80	44.59	44.78	G
Mrk 78	0.037	0.13	0.56	1.11	1.13	44.44	44.63	G
Mrk 266	0.028	0.23	0.98	7.34	11.1	45.07	45.03	I
Mrk 273	0.038	0.24	2.28	21.7	21.4	45.75	45.69	G
Mrk 463	0.051	0.51	1.58	2.18	1.92	45.00	45.34	G
Mrk 477	0.038	0.13	0.51	1.31	1.85	44.58	44.70	G
Mrk 686	0.014	<0.11	0.13	0.57	1.79	43.49	43.43–43.56	I
NGC 1068	0.004	39.70	85.04	176.2	224.0	44.72	44.96	G
NGC 3227	0.004	0.67	1.76	7.83	17.6	43.46	43.49	I
NGC 5033	0.003	0.95	1.15	13.8	43.9	43.54	43.48	I
NGC 5135	0.014	0.64	2.40	16.9	28.6	44.84	44.81	G
NGC 5929	0.008	0.43	1.62	9.14	13.7	44.06	44.06	G, I

Note. — Column (1): Object. Column (2): Redshift. Column (3)–(6): f_{12} , f_{25} , f_{60} , and f_{100} are *IRAS FSC* fluxes at $12\mu\text{m}$, $25\mu\text{m}$, $60\mu\text{m}$, and $100\mu\text{m}$, respectively. Column (7): Logarithm of far-infrared (40–500 μm) luminosity in ergs s^{-1} calculated with $L_{\text{FIR}} = 1.4 \times 2.1 \times 10^{39} \times D(\text{Mpc})^2 \times (2.58 \times f_{60} + f_{100})$ [ergs s $^{-1}$] (Sanders & Mirabel 1996). Column (8): Logarithm of infrared (8–1000 μm) luminosity in ergs s^{-1} calculated with $L_{\text{IR}} = 2.1 \times 10^{39} \times D(\text{Mpc})^2 \times (13.48 \times f_{12} + 5.16 \times f_{25} + 2.58 \times f_{60} + f_{100})$ [ergs s $^{-1}$] (Sanders & Mirabel 1996). Column (9): G: sources studied by Gonzalez Delgado et al. (2001). I: sources studied by Ivanov et al. (2000).

Table 2. Observing Log.

Object	Date (UT)	Integration Time (sec)	Standard Star			
			Star Name	<i>L</i> -mag	Type	T _{eff} (K)
IC 3639	2001 Apr 8	1920	HR 5212	4.8	F7V	6240
Mrk 34	2001 Apr 9	2520	HR 4112	3.4	F8V	6200
Mrk 78	2001 Apr 9	1728	HR 3028	4.8	F6V	6400
Mrk 266SW	2001 Apr 9	2160	HR 4767	4.8	F8V–G0V	6000
Mrk 273	2000 Feb 20	2560	HR 4761	4.8	F6–8V	6200
Mrk 463	2000 Jun 13	800	HR 5243	4.9	F6V	6400
Mrk 477	2001 Apr 9	2592	HR 5581	4.3	F7V	6240
Mrk 686	2001 Apr 9	2400	HR 5423	4.7	G5V	5700
NGC 1068	1995 Nov 15	640	HR 8781	2.6	B9V	10700
NGC 3227	2001 Apr 8	1050	HR 3650	4.6	G9V	5400
NGC 5033	2001 Apr 8	2280	HR 5423	4.7	G5V	5700
NGC 5135	2001 Apr 8	2160	HR 5212	4.8	F7V	6240
NGC 5929	2001 Apr 9	2064	HR 5581	4.3	F7V	6240

Table 3. Our Spectro-photometric *L*-band Magnitudes and Comparisons with Aperture Photometry at *L* in the Literature.

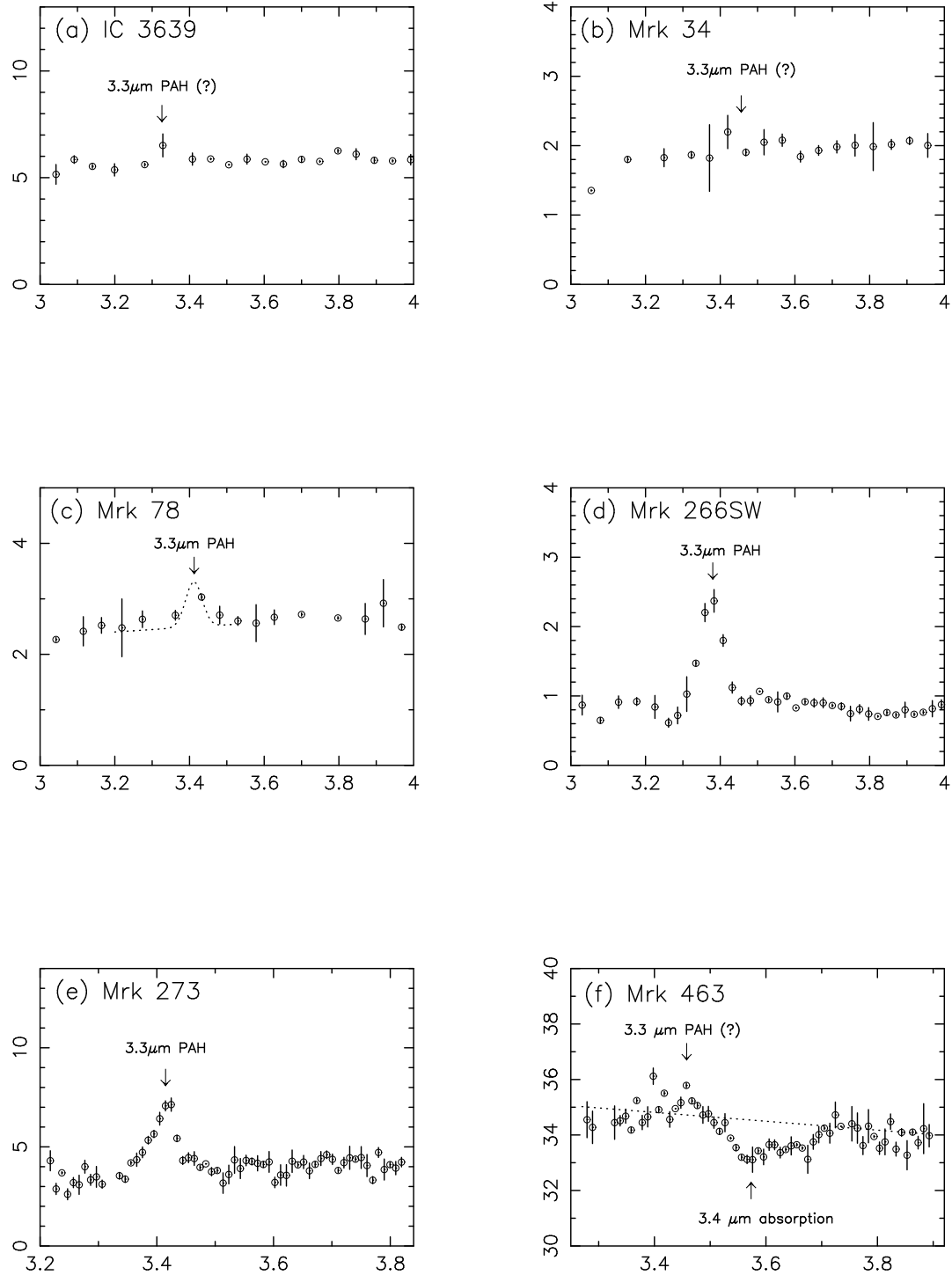
Object (1)	Magnitude		
	(our data) (2)	(literature) (3)	Reference (4)
IC 3639	10.2 (1''.2 \times 5'')	10.4 (6'')	G
Mrk 34	11.3 (1''.2 \times 4'')	11.1 (8''.5)	R
Mrk 78	11.0 (1''.2 \times 5'')	11.0 (5''.9)	R
Mrk 266SW	12.1 (1''.2 \times 5'')	11.5 (8''.6)	I
Mrk 273	10.5 (1''.2 \times 10'')	10.5 (5'')	Z
Mrk 463	8.2 (1''.2 \times 7'')	8.2 (4'')	M
Mrk 477	11.1 (1''.2 \times 4'')	11.8 (6'')	L
Mrk 686	11.0 (1''.2 \times 5'')	11.2 (5''.4)	I
NGC 1068	4.8 (3''.8 \times 3''.8)	4.8 (3'')	MA
NGC 3227	9.5 (1''.2 \times 4'')	9.0 (8''.6)	I
NGC 5033	10.7 (1''.2 \times 5'')	9.5 (8''.6)	I
NGC 5135	10.1 (1''.2 \times 6'')	9.7 (6'')	G
NGC 5929	11.6 (1''.2 \times 5'')	10.8 (5''.4)	I

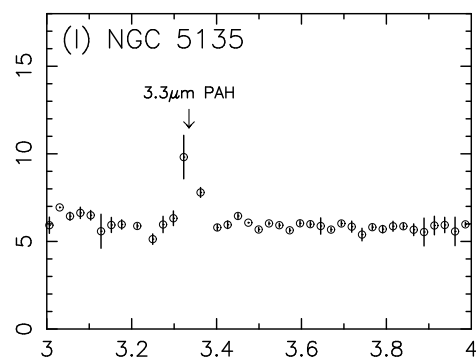
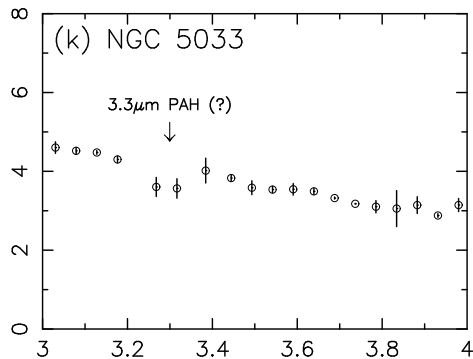
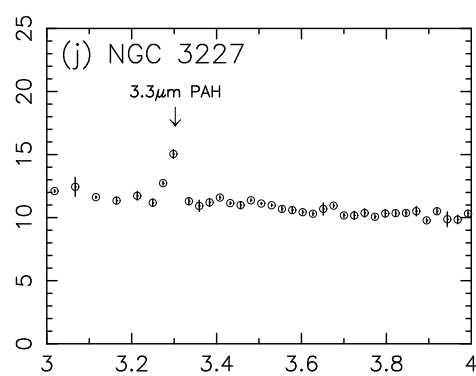
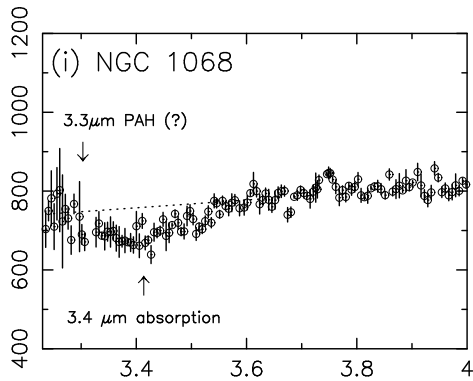
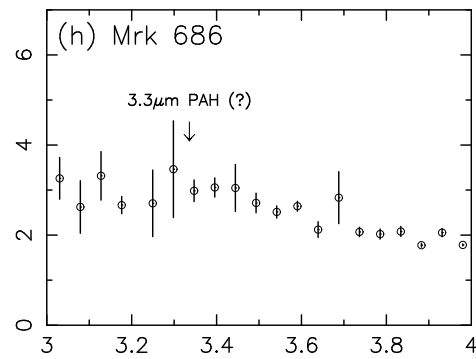
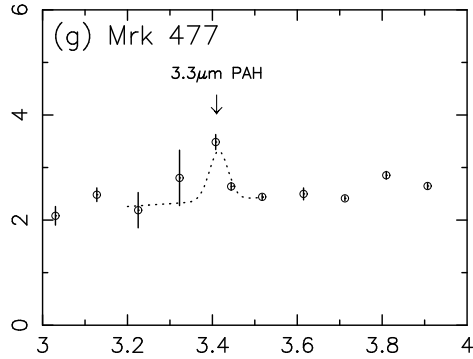
Note. — Column (1): Object. Column (2): Our spectro-photometric magnitude at *L*. Column (3): Aperture photometric *L*-band magnitude from the literature. Column (4): References for the aperture photometry. G: Glass and Moorwood (1985), I: Ivanov et al. (2001), L: Lawrence et al. (1985), M: Mazzarella et al. (1991), MA: Marco & Alloin (2000), R: Rieke (1978), Z: Zhou, Wynn-Williams, & Sanders (1993).

Table 4. The Properties of the $3.3\text{ }\mu\text{m}$ PAH Emission Feature.

Object (1)	$f_{3.3\text{PAH}}$ ($\times 10^{-14}$ ergs s^{-1} cm^{-2}) (2)	$L_{3.3\text{PAH}}$ ($\times 10^{39}$ ergs s^{-1}) (3)	$L_{3.3\text{PAH}}/L_{\text{IR}}$ ($\times 10^{-3}$) (4)	rest EW $_{3.3\text{PAH}}$ ($\times 100$ nm) (5)
IC 3639	<4.9	<11.3	<5.2 $\times 10^{-2}$	<8.5 $\times 10^{-2}$
Mrk 34	<0.33	<17.5	<2.9 $\times 10^{-2}$	<1.6 $\times 10^{-2}$
Mrk 78	3.9 ± 1.0	108 ± 27	2.5×10^{-1}	$1.5 \pm 0.4 \times 10^{-1}$
Mrk 266SW	8.5 ± 0.5	133 ± 7	1.2×10^{-1}	$8.7 \pm 0.5 \times 10^{-1}$
Mrk 273	14.5 ± 0.7	422 ± 19	8.7×10^{-2}	$3.5 \pm 0.2 \times 10^{-1}$
Mrk 463	<3.0	<159	<7.4 $\times 10^{-2}$	<8.1 $\times 10^{-3}$
Mrk 477	5.1 ± 0.7	151 ± 21	3.0×10^{-1}	$2.2 \pm 0.3 \times 10^{-1}$
Mrk 686	<3.3	<12	<4.6 $\times 10^{-1}$	<1.2 $\times 10^{-1}$
NGC 1068	<86.7	<26.7	<2.9 $\times 10^{-2}$	<1.2 $\times 10^{-2}$
NGC 3227	16.6 ± 1.3	5.1 ± 0.4	1.7×10^{-1}	$1.4 \pm 0.1 \times 10^{-1}$
NGC 5033	<0	<0	<0	<0
NGC 5135	15.3 ± 2.8	58 ± 11	9.1×10^{-2}	$2.4 \pm 0.4 \times 10^{-1}$
NGC 5929	<2.5	<3.0	<2.7 $\times 10^{-2}$	<1.4 $\times 10^{-1}$

Note. — Column (1): Object. Column (2): Observed $3.3\text{ }\mu\text{m}$ PAH flux. Column (3): Observed $3.3\text{ }\mu\text{m}$ PAH luminosity. Column (4): Observed $3.3\text{ }\mu\text{m}$ PAH to infrared luminosity ratio in units of 10^{-3} , the typical value for starburst galaxies. Column (5): Rest frame equivalent width of the $3.3\text{ }\mu\text{m}$ PAH emission in units of 100 nm, approximately the typical value for starburst galaxies (~ 120 nm).





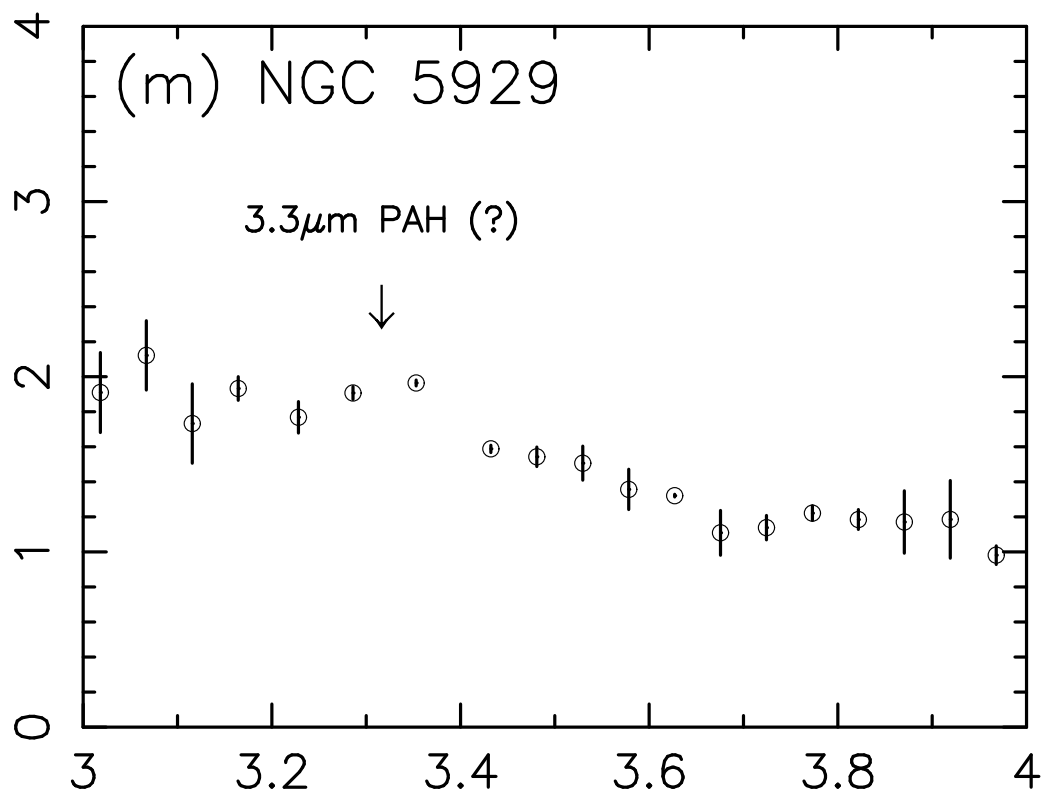


Fig. 1.— $3-4 \mu\text{m}$ spectra of the 13 Seyfert 2 nuclei. The abscissa and ordinate are the observed wavelength in μm and F_λ in $10^{-15} \text{ W m}^{-2} \mu\text{m}^{-1}$, respectively. For Mrk 78 and Mrk 477, the dotted lines are the best fit for the $3.3 \mu\text{m}$ PAH emission feature. For Mrk 463 and NGC 1068, the dotted lines are the adopted continuum levels, with respect to which the optical depths of the $3.4 \mu\text{m}$ dust absorption are measured.

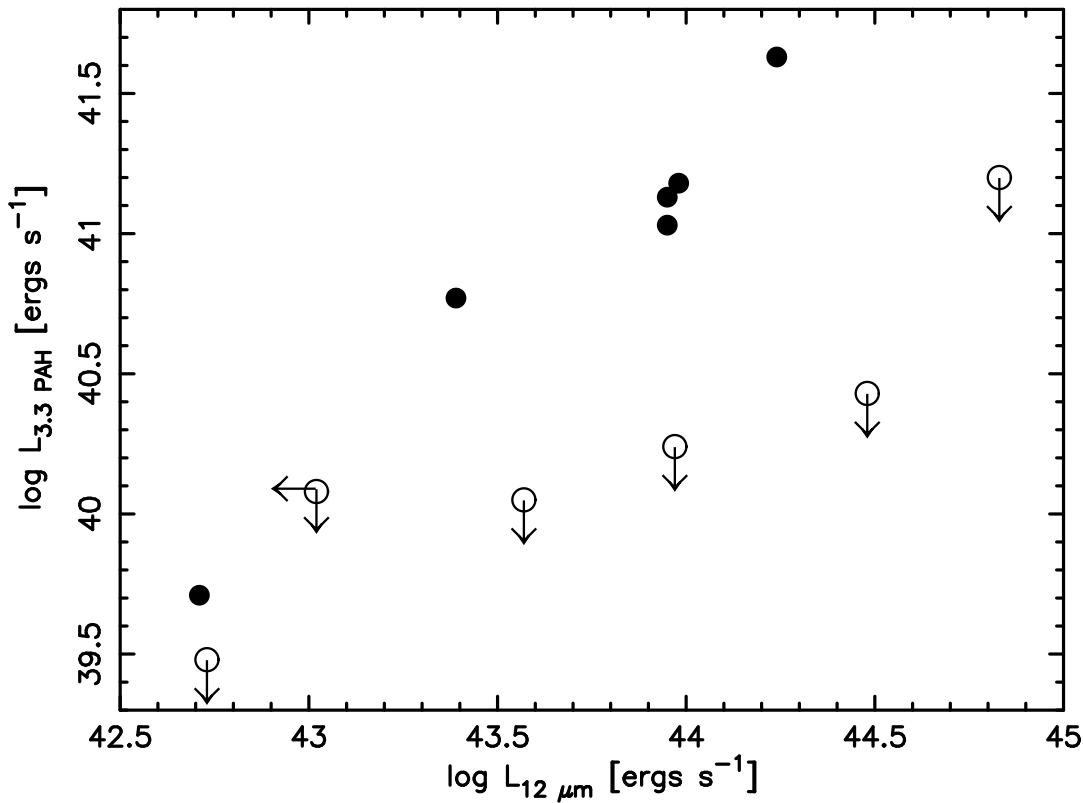


Fig. 2.— The relation between the logarithm of the $12 \mu\text{m}$ luminosity (νF_ν) in ergs s^{-1} (abscissa) and the $3.3 \mu\text{m}$ PAH emission luminosity in ergs s^{-1} measured with our slit spectra (ordinate). The filled and open circles are Seyfert 2 nuclei with detected and non-detected $3.3 \mu\text{m}$ PAH emission, respectively. NGC 5033 is excluded because no meaningful upper limit for the $3.3 \mu\text{m}$ PAH emission is given.